IEEE Access
Multidisciplinary | Rapid Review | Open Access Journal

Received March 1, 2021, accepted March 21, 2021, date of publication March 24, 2021, date of current version April 1, 2021.

Digital Object Identifier 10.1109/ACCESS.2021.3068374

Energy Efficiency Analysis and Optimization of Industrial Processes Based on a Novel Data Reconciliation

SEN XIE[1,2], HUAIZHI WANG[1], (Member, IEEE), AND JIANCHUN PENG[1]
[1]College of Mechatronics and Control Engineering, Shenzhen University, Shenzhen 518060, China
[2]College of Physics and Optoelectronic Engineering, Shenzhen University, Shenzhen 518060, China

Corresponding author: Huaizhi Wang (wanghz@szu.edu.cn)

This work was supported in part by the National Natural Science Foundation of China under Grant 61903257, in part by the International Cooperative Research Project of Shenzhen under Grant GJHZ20180928160212241, and in part by the Fundamental Research Project of Shenzhen under Grant JCYJ20190808165201648.

ABSTRACT The energy management and energy efficiency optimization are of particularly significant for promoting the sustainable development of industrial processes. However, industrial raw data with uncertain, relevant and inaccuracy characteristics influence the reliability and accuracy of energy efficiency analysis and optimization modeling. Therefore, an energy efficiency analysis and optimization method based on a novel data reconciliation (DR) integrating Gaussian mixture model (GMM) and mutual information (MI) is put forward. First, the material flow information with multiple data characteristics corresponding operation modes is divided through the GMM. Moreover, the novel data reconciliation model integrated with critical variable and mutual information is established considering time-scale redundancy information in different modes, then the comprehensive data reconciliation result is evaluated by the hypothesis testing. Furthermore, the reconciled data is applied to analyze the exergy balance and built the energy efficiency optimization model with multi-objective for a case study of industrial evaporation process. Finally, simulation case and industrial application case are used to analyze and discuss, and the results show that the validity and applicability of the proposed approach are illustrated in energy saving potential which is about 14.81%.

INDEX TERMS Energy efficiency analysis, energy optimization, data reconciliation, Gaussian mixture model, mutual information, industrial processes.

I. INTRODUCTION

In the face of the rapid development industrialization and urbanization, energy conversion and management of industrial processes are critical for the sustainable development [1]. The effective and credible energy efficiency analysis and optimization modeling is the key ways for achieving the economic and environmental goals [2]. Nevertheless, the actual industrial production is affected by many uncertain factors, such as diverse material, process parameter variation, poor production environment and market demand [3]. Meanwhile, industrial plants rely on a large amount inputs of production factors to achieve revenue grow, it is still an extensive management mode in terms of energy utilization [4]. In China, there are enormous challenges and room for improvement in energy management. The reduction of energy consumption and the improvement of energy efficiency have become a long-term target [2]. Meanwhile, energy efficiency optimization as an effectiveness way to ensure high energy efficiency has received attention throughout industry and academic in recent years [5]. Therefore, accurate energy efficiency analysis and optimization is conductive for increasing economic benefits, promoting production management, and reducing environmental pollution in industrial processes.

Up to now, energy analysis methods [6] have emerged by utilizing energy characteristics and conversion laws of various processes or production equipment in industrial process to evaluate the energy utilization effectively [7]. Generally speaking, existing energy analysis methods are divided into three types: enthalpy analysis, entropy analysis and exergy analysis. The enthalpy analysis method uses the comprehensive energy consumption of the device as the evaluation

The associate editor coordinating the review of this manuscript and approving it for publication was Wen-Sheng Zhao.

criterion to analyze the energy utilization in quantity according to the first law of thermodynamics [8]. However, not all processes that satisfy the energy conservation can be realized, and the second law of thermodynamics should be also satisfied. The disadvantage of enthalpy analysis method is that the amount of energy is simply used to evaluate the energy consumption, and the problem of equivalent conversion of energy in the transmission process is ignored. Especially for heat transfer, the process energy level will change with the change of energy thermodynamic parameters (temperature, pressure, etc.) inevitably. Therefore, the enthalpy analysis method has certain limitations, which cannot grasp the keys in the energy-saving technology transformation and cannot reflect the energy consumption truly.

Moreover, the entropy analysis method reflects the change of energy level by using the variation trend of entropy on the basis of the second law of thermodynamics [9]. The smaller the entropy increase, the smaller the loss, and the higher the efficiency [10]. Nevertheless, the entropy as a physical quantity, reflecting the internal chaos and disorder state of material, cannot be measured with instruments directly but can only be calculated. Thus, entropy analysis method describes the change of energy quality, but it is not intuitive.

Furthermore, exergy analysis method focuses on that the degree of deviation between the system and the environmental parameters is used to measure the energy which can be utilized or transformed by the system [11]. Based on the environmental reference state model, exergy analysis method describes the variations and differences of energy quality and quantity [12]. Moreover, the property, loss and conversion efficiency of energy are analyzed through the energy analysis method based on exergy, so as to find out the link with the greatest exergy loss and evaluate the energy consumption of each link of the system [13]. In general, the energy analysis methods based on the exergy calculation, including white box analysis model [14], heat exchange network synthesis technology [15], gray box analysis model [16], exergy economic method and pinch point technology [17], etc., have been successfully applied in industrial process energy analysis, such as boiler [18], atmospheric distillation unit [19], galvanizing annealing furnace [20], asphalt plant's rotary dryer [21], polygeneration energy system [22], energy comprehensive utilization in solar heat pump system [23], and other equipment and process energy analysis. At present, the exergy efficiency and exergy destruction rate as the main indexes are calculated and evaluated, and the operating parameters were optimized to improve overall production system performance by minimizing total cost rate and maximizing exergy efficiency [24], [25]. Besides, exergy analysis has been used for energy consumption evaluation of industrial equipment, for instance, waste heat recovery of biodiesel-fed diesel engine [26] and oxyfuel gas turbine [27]. In addition to the equipment-level energy consumption evaluation, exergy analysis has also been applied in the whole process of industrial production like cogeneration nuclear energy cycle system [28] and calcination process of lime industry [29]. The main causes of thermodynamic loss and the exergy distribution of the relevant component are identified and evaluated, and then the exergy efficiency is improved through controlling key process variables. In fact, exergy defined from the two aspects of quantity and quality is used to evaluate the energy, and it can provide a good reference for energy analysis and optimization in industrial production.

Furthermore, improvement of energy efficiency is a conductive way to achieve economic growth and friendly environment. In the recent years, energy efficiency optimization methods have been concerned highly [30]. The energy cost is reduced in a variety of ways, such as energy-efficiency scheduling integrating process optimization [31], using key performance indicators which relate to energy [32]. Moreover, aiming at the construction of the energy efficiency optimization model, production information such as historical working condition is introduced to further improve the model structure to meet the actual production demand [33]. Besides, to improve the effectiveness of energy efficiency optimization modeling, it can construct knowledge-based mechanism to ensure the convergence of optimization algorithm [34]. In addition, it can also make use of data analysis methods such as data envelopment analysis [35] and improved Contourlet neural network [36] to improve the optimization performance for guaranteeing the high energy efficiency and reasonable energy efficiency assessment strategy. The previous works provide motivation and inspiration for the energy efficiency optimization of the evaporation process in this paper.

However, firstly, due to uncertain fluctuation of feed condition and changes in production demands, the production process has multiple stable working states, that is, multiple production modes. There are obvious differences in data characteristics under different production modes, which leads to the fact that single global modeling strategy cannot meet the effectiveness of energy efficiency analysis and optimization. In addition, the measured data in the industrial processes interfered by the detection instrument and harsh environment, has noise characteristics and multiple dimensions. Thus, the material flow information cannot inflect the actual production, which is detrimental to assess energy efficiency accurately. Moreover, some variables of intermediate equipment are unmeasured for the industrial processes, resulting in insufficient data redundancy and partial material flow information which is missing. Hence, recognizing the above challenges, to avoid the limitations for the existing energy efficiency optimization methods, the main contributions of this paper are summarized: (1) In order to avoid comprehensive and accurate of energy efficiency optimization being affected by the diversity of data characteristics, this paper divides the industrial production process with multi-features material flow information into several sub-mode by the Gaussian mixture model. (2) Data reconciliation technology is used to obtain the complete and reliable process monitoring information and the critical

variable is introduced to improve data redundancy of local data reconciliation modeling in each mode. Meanwhile, mutual information is applied to characterize the nonlinear correlation for reconciliation model, and the hypothesis testing is applied to evaluate the reconciliation results. (3) Based on the process analysis and raw data preprocessing for a case study, the exergy is analyzed and calculated to construct a multi-objective optimization model based on the maximum exergy efficiency and minimum steam consumption, further reduce the unnecessary exergy loss and improve the energy efficiency for evaporation process of industrial production.

The rest of this paper is organized as follows. The novel data reconciliation on the basis of GMM and mutual information is presented in Section II. Section III elaborates a case study for energy efficiency optimization modeling with exergy balance analysis of the evaporation process. Section IV presents experimental simulation results analysis and industrial application. We conclude this study in Section V.

II. THE NOVEL DR BASED ON GMM AND MUTUAL INFORMATION

To ensure the feasibility of energy efficiency optimization of the industrial processes, superior data quality is especially significant. In fact, for the industrial processes, under the influence of the uncertainty fluctuation of production conditions and product demand adjustment, the data features, such as mean value, variance and correlation coefficient are obvious different. This indicates that the different production modes exist and the effectiveness of reconciliation model is affected by the single global data reconciliation modeling method. Furthermore, the measurement error is not only from the sensor, but also caused by feedback control, external interference and model error. The measurement error may have nonlinear correlation. Besides, the long-process industrial production is composed of many production equipment, and the material flow information of intermediate equipment is absence due to running environment and economic conditions. It results in the insufficient data redundancy. Consequently, above practice issues are considered, and according to GMM and mutual information, a novel data reconciliation scheme with multi-features material flow and time-scale redundancy information is established.

In this section, we review the existing data reconciliation approaches and propose a generic data reconciliation with time-scale redundancy information firstly. Then, the detailed processes of the novel data reconciliation scheme are described.

A. PROPOSED GENERIC DR MODEL

Data reconciliation originally proposed by Kuehn and Davidson [37] minimizes the errors from measured data based on the Lagrange multiplier method. Inspired by Kuehn's work, a lot of diversified data reconciliation models have emerged. From the early linear data reconciliation to the bilinear data reconciliation research, it gradually develops to the nonlinear data reconciliation for more and more complex research object [38], [39]. In fact, data redundancy is a significant prerequisite for data reconciliation. The adaptability and accuracy of the data reconciliation model are limited when the measured data with low redundancy. Thus, it is possible to improve data redundancy by introducing constraints, such as equations of pressure drop, efficiency of turbine internal, steam flow rate, and heat flow characteristics [40], even equipment characteristic [41], [42], or changing the data reconciliation model structure [43]. Furthermore, for the process industry with multi-equipment cascade and uncertainties, the research of data reconciliation method integrating multiple sub-reconciliation models has become a trend [44], [45].

Generally, the data reconciliation is limited to use the measured variables at the same time to determine the reconciliation model. However, in the long-process industrial production process with connected multi-equipment, the key material flow information of intermediate equipment cannot be detected due to the environmental restrictions, resulting in insufficient data redundancy. Therefore, the critical variable is introduced in this paper to improve the monitoring accuracy by using the time redundancy information of continuous steady-state data.

In detail, the critical variable is basically constant in a short time or a quasi-steady state. Thus, the critical variable is regarded as a measured variable in the novel data reconciliation modeling. Nevertheless, the measured value of the critical variable is unknown, such that the initial measured value is given according to the actual experience, and the reconciled data is regarded as the measured data of the next iteration. Moreover, the critical variable iterates and gradually converges under the constraint equations. Hence, a proposed generic data reconciliation model is expressed following,

$$\begin{aligned}\min \psi = &\sum_{i=1}^{l}\sum_{j=1}^{n}\left(\frac{x_{ij,t}-\hat{x}_{ij,t}}{\sigma_i}\right)^2 \\ &+\sum_{s=1}^{r}\sum_{j=1}^{n}\left(\frac{\widehat{y}_{sj,t}-\widehat{y}_{sj,t-1}}{\widehat{\sigma}_s}\right)^2 \qquad (1)\\ s.t.\ &\mathbf{H}\left(\hat{\mathbf{X}},\widehat{\mathbf{Y}},\mathbf{U}\right)=0\\ &\hat{x}_{\mathrm{L}}^{i}\le\hat{x}^{i}\le\hat{x}_{\mathrm{U}}^{i}\quad i=1,2,\ldots,l\\ &\widehat{y}_{\mathrm{L}}^{s}\le\widehat{y}^{s}\le\widehat{y}_{\mathrm{U}}^{s}\quad s=1,2,\ldots,r\\ &u_{\mathrm{L}}^{q}\le u^{q}\le u_{\mathrm{U}}^{q}\quad q=1,2,\ldots,p \qquad (2)\end{aligned}$$

where t and t-1 are the present and the previous time, respectively; $x_{ij,t}$ and $\hat{x}_{ij,t}$ are the measurement and reconciliation of the jth sample for the ith measurement variable, respectively; $\widehat{y}$ is the critical variable; σ is the standard deviation; l, r, p and n are the number of the measurement variables, the critical variables, the unmeasured variables and the samples, respectively; u is the unmeasured variables. The redundancy characteristic of the critical variable which is essentially invariant on the time scale is used to improve the redundancy information of the monitoring system.

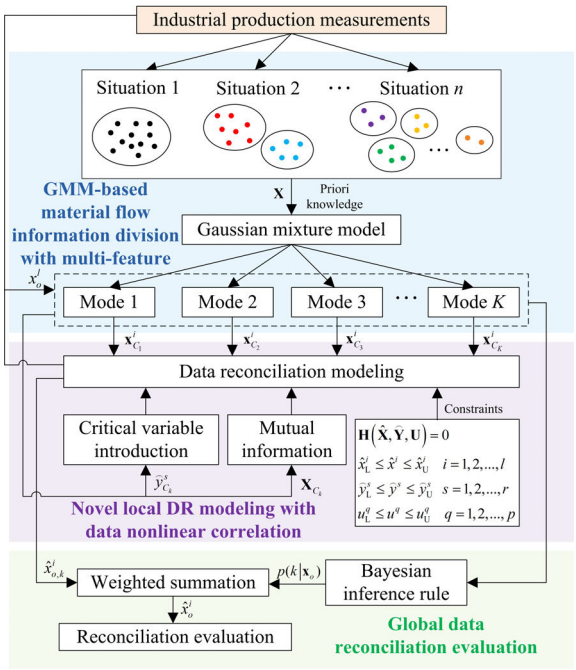

FIGURE 1. Structure of the proposed novel data reconciliation scheme.

B. A NOVEL DR SCHEME BASED ON GMM AND MUTUAL INFORMATION

Traditional weighted least square method-based data reconciliation provides the possibility to improve the data quality in several applications. However, it fails to handle the process data with multi-mode, nonlinear and low redundancy, which causes biased reconciliations and thus influences the accuracy of the process modeling, optimization and control severely. Therefore, a novel DR scheme based on GMM and mutual information is proposed to overcome the deficiencies of traditional weighted least square method-based data reconciliation. It consists of three steps, first, the multi-features material flow information is divided to the different operation modes by GMM. Then, the critical variable and mutual information are introduced to determine the novel data reconciliation model. Furthermore, the hypothesis testing is leveraged to evaluate the global data reconciliation results.

1) GMM-BASED MATERIAL FLOW INFORMATION DIVISION WITH MULTI-FEATURES

It is affected by the changeable operation condition and the product demand, the data features, including the mean value, the variance and the correlation coefficient are multifarious, which lead to the fact that the probability density distribution of process data in multiple mode may overlap. Hence, the material flow information with multi-features is divided through GMM, and the process data is ensured in different mode. GMM as an appropriate tool to determine the data distribution can describe mixed probability density distribution and represent any complex probability density function with enough gaussian components [46], [47]. Yu *et al.* improved adaptive kernel partial least squares regression using the finite mixture model based GMM and the multi-channel GMM based for quality prediction and soft sensor [48], [49]. Sang et al put forward a GMM and discriminant analysis method on the basis of principal components [50]. On this basis, a finite GMM based on Bayesian inference was used to monitor the multi-mode production process [51].

For a measured sample dataset $\mathbf{X} = [\mathbf{x}^1, \mathbf{x}^2, \ldots, \mathbf{x}^m] \in \mathbf{R}^{n\times m}$, where n is the measured samples size, and m is the number of measured variables. Assume K clusters in GMM which is decided through the expert rules or priori knowledge, thus, the process material flow information with multi-features is divided into K local modes. Denote that $\mathbf{X}_{C_k} = [\mathbf{x}^1_{C_k}, \mathbf{x}^2_{C_k}, \ldots, \mathbf{x}^m_{C_k}]$ is the sample set in the kth mode;$\mathbf{x}^i_{C_k} = \left[x^i_{C_k,1}, \ldots, x^i_{C_k,j}, \ldots, x^i_{C_k,n_k}\right]^{\mathrm{T}}$ is the measured data for the ith variable in the kth mode; n_k is the number of samples of the kth mode. Based on multi-mode with multi-features division, the proposed generic DR model of the kth mode is established as,

$$\begin{cases} \min f = \sum_{i=1}^{l}\sum_{j=1}^{n_k} f(x^{ij,t}_{C_k}, \hat{x}^{ij,t}_{C_k}) + \sum_{s=1}^{r}\sum_{j=1}^{n_k} f(\widehat{y}^{sj,t}_{C_k}, \widehat{y}^{sj,t-1}_{C_k}) \\ \quad = \sum_{i=1}^{l}\sum_{j=1}^{n_K} \dfrac{\left(x^{ij,t}_{C_k} - \hat{x}^{ij,t}_{C_k}\right)^2}{\sigma^2_{C_{k,i}}} \\ \quad + \sum_{s=1}^{r}\sum_{j=1}^{n_K} \dfrac{\left(\widehat{y}^{ij,t}_{C_k} - \widehat{y}^{ij,t-1}_{C_k}\right)^2}{\widehat{\sigma}^2_{C_{k,s}}} \\ s.t.\ \mathbf{H}\left(\hat{\mathbf{X}}_{C_k}, \widehat{\mathbf{Y}}_{C_k}, \mathbf{U}_{C_k}\right) = 0 \\ \quad \hat{x}^i_{\mathrm{L}} \le \hat{x}^i_{C_K} \le \hat{x}^i_{\mathrm{U}} \quad i = 1, 2, \ldots, l \\ \quad \widehat{y}^s_{\mathrm{L}} \le \widehat{y}^s_{C_K} \le \widehat{y}^s_{\mathrm{U}} \quad s = 1, 2, \ldots, r \\ \quad u^q_{\mathrm{L}} \le u^q_{C_K} \le u^q_{\mathrm{U}} \quad q = 1, 2, \ldots, p \end{cases} \tag{3}$$

2) NOVEL LOCAL DR MODELING WITH DATA NONLINEAR CORRELATION

Evidently, the measurement errors not only from sensor error but also caused by uncertain factors such as external interference, model error or feedback control, are nonlinear correlation. Thus, the traditional weight least square data reconciliation model which assumes that the measurement errors are independent cannot meet the requirements of reconciliation accuracy. Hence, a novel DR model with data nonlinear correlation is proposed. First, based on the mutual information, DR model including critical variable with data redundancy is determined. Then, the reliability analysis of reconciliation results is realized.

In the light of information entropy, the association degree between two variables is represented to use the mutual information which is an information measurement method [52]. It means that the introduction of one random variable leads to the uncertainty reduction of the other random variable. Therefore, based on introduced critical variable and time-scale information, a novel DR model with data nonlinear

correlation is expressed as

$$\begin{aligned}
&\min_{\hat{x},\tilde{y},u} f \\
&= \sum_{j=1}^{n} \left\{ \left[x_{n,t}^1 - \hat{x}_{n,t}^1 \; x_{n,t}^2 - \hat{x}_{n,t}^2 \; \cdots \; x_{n,t}^l - \hat{x}_{n,t}^l \right] \right. \\
&\quad \cdot \begin{bmatrix} w_{11}^1 & w_{12}^1 & \cdots & w_{1l}^1 \\ w_{21}^1 & w_{22}^1 & \cdots & w_{2l}^1 \\ \cdots & \cdots & \cdots & \cdots \\ w_{l1}^1 & w_{l2}^1 & \cdots & w_{ll}^1 \end{bmatrix} \\
&\quad \left. \cdot \left[x_{n,t}^1 - \hat{x}_{n,t}^1 \; x_{n,t}^2 - \hat{x}_{n,t}^2 \; \cdots \; x_{n,t}^l - \hat{x}_{n,t}^l \right]^{\mathrm{T}} \right\} \\
&\quad + \sum_{j=1}^{n} \left\{ \left[\widehat{y}_{n,t}^1 - \widehat{y}_{n,t-1}^1 \; \widehat{y}_{n,t}^2 - \widehat{y}_{n,t-1}^2 \; \cdots \; \widehat{y}_{n,t}^r - \widehat{y}_{n,t-1}^r \right] \right. \\
&\quad \cdot \begin{bmatrix} w_{11}^2 & w_{12}^2 & \cdots & w_{1r}^2 \\ w_{21}^2 & w_{22}^2 & \cdots & w_{2r}^2 \\ \cdots & \cdots & \cdots & \cdots \\ w_{r1}^2 & w_{r2}^2 & \cdots & w_{rr}^2 \end{bmatrix} \\
&\quad \left. \cdot \left[\widehat{y}_{n,t}^1 - \widehat{y}_{n,t-1}^1 \; \widehat{y}_{n,t}^2 - \widehat{y}_{n,t-1}^2 \; \cdots \; \widehat{y}_{n,t}^r - \widehat{y}_{n,t-1}^r \right]^{\mathrm{T}} \right\} \\
&s.t. \;\; \mathbf{H}\left(\hat{\mathbf{X}}, \widehat{\mathbf{Y}}, \mathbf{U}\right) = 0 \\
&\quad \hat{x}_{\mathrm{L}}^i \le \hat{x}^i \le \hat{x}_{\mathrm{U}}^i \quad i = 1, 2, \ldots, l \\
&\quad \widehat{y}_{\mathrm{L}}^s \le \widehat{y}^s \le \widehat{y}_{\mathrm{U}}^s \quad s = 1, 2, \ldots, r \\
&\quad u_{\mathrm{L}}^q \le u^q \le u_{\mathrm{U}}^q \quad q = 1, 2, \ldots, p
\end{aligned} \tag{4}$$

where $\mathbf{W}_1$ and $\mathbf{W}_2$ represent the mutual information matrix.

3) GLOBAL DATA RECONCILIATION EVALUATION

According to the novel local DR model mentioned before, the similarity between the measured data and the production modes is considered through the calculated probability. Then, local DR result is obtained according to the different model. Finally, the global data reconciliation results are obtained through the weight combination method.

A set of online data sample is represented as $\mathbf{x}_o = [x_o^1, x_o^2, \ldots, x_o^l]$, where for the lth measured variable, x_o^l is the online measurement. According to the Bayesian inference rule, the probability $p(k\,|\mathbf{x}_o)$ is calculated as Eq. (5). Then, the local data reconciliation results of each mode are combined in Eq. (6).

$$p(k\,|\mathbf{x}_o,\,\Omega) = \frac{p(k\,|\Omega)p(\mathbf{x}_o|k,\,\Omega)}{p(\mathbf{x}_o|\Omega)} = \frac{\omega_k f(x\,|\theta_k)}{\sum_{z=1}^{K} \omega_z f(x\,|\theta_z)} \tag{5}$$

$$\hat{x}_o^i = \sum_{k=1}^{K} p(k\,|\mathbf{x}_o)\hat{x}_{o,k}^i \tag{6}$$

where Ω is the total parameters of GMM; θ is the parameters that ensure the Gaussian distribution; $\hat{x}_o^i$ is the global reconciliation result; $\hat{x}_{o,k}^i$ is the reconciliation result of the ith measured variable for the kth mode.

In addition, the objective function value is used to define the reliability evaluation index. If the reconciliation result after an iteration satisfies Eq. (7), the result is reliable.

$$\frac{\psi}{\chi_{1-\alpha,r}^2} \le 1 \tag{7}$$

where $\chi_{1-\alpha,r}^2$ is the $1-\alpha$ quantile of chi square distribution with degree of freedom r; significance level α is 5%; degree of freedom r is the number of redundant variables.

Compared with the reliability evaluation index, if $\psi \le \chi_{1-\alpha,r}^2$, it indicates that there is no gross error in measured variables, that is, there is no fault in the instrument or equipment. If $\psi > \chi_{1-\alpha,r}^2$, the sensor is affected by faults. Moreover, at the beginning of the iteration of the novel data reconciliation method, the critical variable has not yet converged, and the reconciliation results cannot generally meet the Eq. (7).

4) THE FRAMEWORK OF THE NOVEL DR INTEGRATED THE GMM-MI

The structure of the novel DR integrated the GMM-MI is shown in Fig. 1, and the main procedures are displayed as below.

Step 1: Data preparation. The original data is collected according to the measured variables.

Step 2: Based on the GMM, the process material flow information with multi-features is divided into the corresponding running mode.

Step 3: The DR model is established for each mode through the mutual information which describes the nonlinear correlation of variables and the critical variable that improves the data redundancy.

Step 4: The posterior probability that the sample belongs to each mode combines with the reconciliation result from different DR model, and the global reconciliation result is obtained and evaluated by the reliability evaluation index.

III. CASE STUDY: ENERGY EFFICIENCY OPTIMIZATION WITH EXERGY BALANCE ANALYSIS OF THE EVAPORATION PROCESS

Aluminum as the largest consumption of nonferrous metal materials is widely used in construction, military aviation and other industries [53]. The preparation of aluminum requires extraction of alumina which is then electrolyzed. Nevertheless, in China, the shortage of bauxite and the backward industrial production technology lead to the growth of energy consumption and resources and the reduction of international competitiveness in alumina enterprises. Therefore, on the basis of improving data quality, how to guarantee product quality and production efficiency through process optimization and control to reduce energy consumption and environmental pollution is an urgent problem for nonferrous metallurgical enterprises. In this section, first, a schematic description and data analysis is given for the evaporation process. Then, exergy analysis method is carried out for evaluating the energy consumption. Afterwards, multi-objective

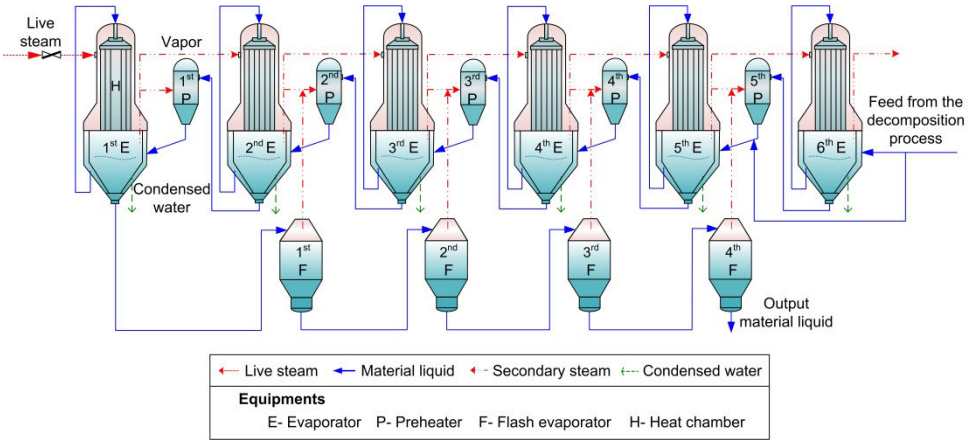

FIGURE 2. The schematic chart of evaporation.

optimization based on exergy evaluation index is implemented for improving energy efficiency in evaporation process.

A. ANALYSIS OF EVAPORATION PROCESS

The evaporation process is an important part to improve the circulating mother liquor concentration through the heated steam in industrial alumina production. It is developed to reduce the discharge of waste lye and thus protect the environment. In fact, the steam consumption is about 48%-52% for the total steam consumption, and the evaporation process becomes the main energy-consuming process in alumina plant. The evaporation process consists of liquid material, steam and condensation water lines which work in parallel. In the reactors, the steam is used to heat the liquid material indirectly. The liquid material is discharged through six evaporators and four flash evaporators. A schematic chart of evaporation is shown in Fig. 2. Actually, the inlet steam and liquid material come from the decomposition process and the thermal power plant, respectively. The uncertain variation of supplied materials and the change in demand of the outlet liquid material concentration, which results in one steady state production is no longer applicable to the actual situation. Furthermore, the data characteristics such as mean value, variance and correlation coefficient of normal process data are obviously different under multiple production running modes. Besides, the measurement error is not only from sensor error, but also may be caused by external interference, model error or feedback control and other uncertain factors.

On the other hand, the actual evaporation process is a long and complex process involving several successive stages, and a large number of detection information for the intermediate equipment are absent, for example the steam and liquid material flow rate, the liquid material concentration, etc. can only be obtained at the inlet and outlet of the whole process. It leads to insufficient process data redundancy. The material flow information is listed in Table 1 ($\times$ is unknown material flow information, O is nonexistent material flow information, and $\surd$ is known material flow information). In addition, the enthalpy of the steam (H) cannot be measured directly, but it is affected by the steam temperature (T_V). Thus, according to the steam and enthalpy data in the enthalpy table of engineering thermodynamics, the coupling relationship between such physical parameters can be expressed in Eq. (8) through the least square fitting method.

$$H = 2495 + 1.961T_V - 0.002128T_V^2 \tag{8}$$

Actually, the outlet liquid material that satisfies the production requirement is obtained through controlling the process parameters and regulating the temperature distribution. However, normally, the production operating often depends on the experience of the operators. Obviously, this is manual motivation and generally excessive energy consumption. Therefore, in order to achieve green and efficient production, improve energy efficiency, it is essential to ensure the accuracy and completeness of process data before energy consumption optimization, which is conductive to improve the effectiveness of the process modeling, energy consumption optimization and production control.

B. ENERGY ANALYSIS WITH EXERGY

The exergy analysis is to recognize the inappropriate energy utilization, expose the reasons and quantities of exergy loss, and adopt energy-saving measures further. In the exergy analysis for the evaporation process, the impact of pressure loss is ignored, and only the thermal energy and chemical energy in liquid material and steam is concerned. The exergy of the evaporation process is divided that one is the exergy of condensed water and steam, and the other is the exergy of liquid material. As the evaporation process is a physical reaction process, the chemical exergy of liquid material is not considered to calculate exergy, but only the physical exergy of condensed water, steam and liquid material are calculated.

The physical exergy of liquid material is expressed as:

$$e_x = (h_e - h_{e0}) - T_0 (s_e - s_{e0}) \tag{9}$$

TABLE 1. The material flow information for the evaporation process.

Material flow information	Pressure	Temperature	Flow rate	Density	Concentration	Thermal enthalpy	Specific heat capacity
Feed	O	√	√	×	√	O	×
Live steam	√	√	√	O	O	×	O
Secondary steam	√	√	×	O	O	×	O
Outlet liquid material	×	√	√	O	O	O	×
Secondary steam of the 4th F	√	√	×	O	O	×	O
Outlet liquid material of the 4th F	O	√	√	×	√	O	×
Condensed water	O	√	×	√	√	O	√

where h_e and s_e are enthalpy and entropy; h_{e0} and s_{e0} are enthalpy and entropy in reference environment; T_0 is temperature in reference environment.

Here, the thermodynamic data of water and steam obtained by the IAPWS-IF97 model is adopted to calculate exergy of water and steam [54]. However, the ingredient of liquid material is complex and its enthalpy and entropy have no corresponding thermodynamic properties to be checked. Therefore, the Eq. (9) is derived and substituted into the basic thermodynamic equation $dh_e = Tds_e + c_v dP$,

$$de_x = (T - T_0)\, ds_e + c_v dP \tag{10}$$

where c_v is the specific volume.

The calculation formula of specific entropy as follows,

$$ds_e = \left(\frac{\partial s_e}{\partial T}\right)_P dT + \left(\frac{\partial s_e}{\partial P}\right)_T dP \tag{11}$$

where $\left(\frac{\partial s_e}{\partial T}\right)_P = \frac{cp}{T}$, $\left(\frac{\partial s_e}{\partial P}\right)_T = -\left(\frac{\partial c_v}{\partial T}\right)_P$.

Moreover, the Eq. (10) is substituted into the Eq. (11),

$$de_x = cp\left(1 - \frac{T_0}{T}\right) dT + \left[c_v - (T - T_0)\left(\frac{\partial c_v}{\partial T}\right)_P\right] dP \tag{12}$$

Therefore, the physical exergy can be expressed as Eq. (12),

$$\begin{aligned} e_x &= \int_{T_0,P}^{T,P} cp\left(1 - \frac{T_0}{T}\right) dT + \int_{T_0,P_0}^{T_0,P} c_v dP \\ &= cp\left(T - T_0 + T_0 \ln \frac{T_0}{T}\right) \end{aligned} \tag{13}$$

For the stable working conditions, the exergy balance is given as,

$$Ex_{in1} - Ex_{out1} = (Ex_{out2} - Ex_{in2}) + SI \tag{14}$$

The Eq. (14) represents that the heat absorbed by the cold liquid material increases from Ex_{in2} to Ex_{out2} for heat exchanger, and the heat released by the hot liquid material decreases from Ex_{in1} to Ex_{out1}. The exergy loss SI is divided into internal irreversible exergy loss of heat exchange I_c which is the exergy from the condensed water and steam exported the equipment or the evaporation process, and external irreversible exergy loss I_{sr} which is the exergy between the cold and the hot liquid on the inside and outside of the heating tube in the heat transfer process.

Nevertheless, the exergy loss as an absolute variable is unable to compare the degree of exergy utilization in process or equipment under different operating conditions. Thus, it is more appropriate for the exergy efficiency η_{ex} to show the operational efficiency of the equipment, as follows,

$$\eta_{ex} = \frac{E_{effective}}{E_{in}} \times 100\% \tag{15}$$

where $E_{effective}$ is the effective exergy of the system or equipment; E_{in} is exergy supplied to the system or equipment.

1) EXERGY ANALYSIS OF EVAPORATOR

In detail, the exergy flow balance of the ith evaporator is formulated as,

$$E_{vsi-1} + E_{vci} + E_{vfi-1} + E_{mii+1} = E_{voi} + E_{wwi} + E_{moi} + I_{zi} \tag{16}$$

where E_{vsi-1} is the exergy for the secondary steam of the $(i-1)$th evaporator; E_{vci} is the exergy for the flash steam of the ith condensation tank; E_{vfi-1} is the exergy for the steam of the flash evaporator; E_{mii+1} is the exergy for the inlet liquid material; E_{wwi} is the exergy for the condensate water; E_{voi} is the exergy for the secondary steam of the ith evaporator; E_{moi} is the exergy for the outlet liquid; I_{zi} is the exergy loss for the ith evaporator.

2) EXERGY ANALYSIS OF FLASH EVAPORATOR

For the flash evaporators, the exergy balance equations are expressed as,

$$E_{mol} = E_{mf1} + E_{vf1} + I_{s1} \tag{17}$$

$$E_{mf1} = E_{mf2} + E_{vf2} + I_{s2} \tag{18}$$

$$E_{mf2} = E_{mf3} + E_{vf3} + I_{s3} \tag{19}$$

$$E_{mf3} = E_{mo} + E_{vf4} + I_{s4} \tag{20}$$

where for the 1st evaporator, the 1st, the 2nd, the 3rd and the 4th flash evaporator, $E_{mol}, E_{mf1}, E_{mf2}, E_{mf3}, E_{mo}$ are the exergy of the outlet liquid material, respectively; $E_{vf1}, E_{vf2}, E_{vf3}, E_{vf4}$ are the exergy of the flash steam for the 1st, the 2nd, the 3rd and the 4th flash evaporator, respectively; $I_{s1}, I_{s2}, I_{s3}, I_{s4}$ are the exergy loss for the first, the second, the third and the fourth flash evaporator, respectively.

C. ENERGY EFFICIENCY OPTIMIZATION BASED ON PERFORMANCE INDICATOR

Based on the problem that field workers operate roughly at the cost of a large amount of energy consumption for ensuring the concentration of the outlet liquid material, an energy efficiency optimization approach with multi-objective is put forward to reduce the energy consumption as low as possible, maintain production quality and improve energy efficiency.

1) HYPOTHESIS

In order to reduce the mathematical modeling uncertainty under optimal operation, the following assumptions are made:

(a) The flow of liquid material is assumed to be steady flow, and the steam is evenly distributed.

(b) Non-condensable gas is almost nonexistent, and secondary steam and live steam are saturated.

(c) The change of solute mass in the evaporator caused by scaling is ignored.

2) OBJECTIVE FUNCTION

In evaporation process, the energy efficiency optimization is to ensure that the outlet liquid material concentration meets the production requirements with the minimum energy consumption on the basis of the equipment operation capacity and the process constraints. Meanwhile, energy conservation and consumption reduction are to decrease the amount of the steam, reduce the unnecessary energy loss, and improve the energy usage efficiency.

Actually, the steam-water ratio (per mass units of water evaporated by the mass unit of live steam) as an important technical indicator of evaporation process, the larger the steam-water ratio, the more steam needed to evaporate a ton of water, and the higher the steam consumption. In addition, compared with the exergy loss rate, improving the exergy efficiency is conductive to guarantee the low energy consumption. Hence, the objective functions of energy consumption optimization are shown as follows,

$$\min\ J_1 = \min\left(1-\eta_{ex}\right) = \min\left(1-\frac{F_4^s\rho_4^s e_{m_4^s}}{V_0 e_{V0}+F_0\rho_0 e_{m0}}\right) \tag{21}$$

$$\min\ J_2 = \min\left(\frac{V_0}{W_z}\right) = \min\left(\frac{V_0}{F_0\rho_0\left(1-C_0\rho_4^s/C_4^s\rho_0\right)}\right) \tag{22}$$

where for the feed of the process, F_0 and ρ_0 are flow rate and concentration; for the outlet liquid of the 4th flash evaporator, F_4^s and ρ_4^s are flow rate and concentration; V_0 is the live steam flow rate; for the whole evaporation process, the unit exergy of the feed, the unit exergy of the live steam, $e_{m_4^s}$, e_{m0}, e_{V0} are unit exergy for the outlet liquid material, respectively.

According to the reconciliation processing results, the liquid material density is determined by the concentration, as shown,

$$\rho = 1035.425 + 2.688C_{Al_2O_3} + 1.175C_{NaOH} - 2.1C_{Na_2CO_3} \tag{23}$$

where ρ is the density for the liquid material (kg/m^3); $C_{Al_2O_3}$, C_{NaOH}, $C_{Na_2CO_3}$ are the concentration for the aluminium oxide, the sodium hydroxide, the sodium carbonate (g/L), respectively.

3) CONSTRAINTS

The operation parameters should be limited the feasible region to satisfy the equipment capacity and technical requirements, that is, to satisfy process constraint conditions, including mechanism model constraints, live steam flow rate constraint, live steam temperature constraint, feed flow rate constraint, and heat transfer temperature difference constraint.

a: THE CONSTRAINT OF MECHANISM MODEL

The secondary steam generated by the evaporator is supplied to the preheater, and the inlet liquid material of the evaporator comes from the preheater. Besides, evaporator, preheater and condensation water tank as a whole unit, are used for modeling and research of mechanism. The mechanism models are,

$$F_iC_i = F_0C_0(i=1,2,3,4) \tag{24}$$

$$F_5C_5 = F_{02}C_0 + F_6C_6 \tag{25}$$

$$F_6C_6 = F_{01}C_0 \tag{26}$$

$$F_j^sC_j^s = F_0C_0(j=1,2,3,4) \tag{27}$$

$$\left(F_{01}+F_{02}\right)\rho_0 + V_0 = F_4^s\rho_4^s + V_6 \tag{28}$$

$$\left(F_{01}+F_{02}\right)\rho_0 cp_0T_0 + V_0H_0 = F_4^s\rho_4^s cp_4^sT_4^s + V_6H_6 + V_0T_n'cp_w + Q \tag{29}$$

where for liquid material of the evaporator, F, T and cp are flow rate, temperature and specific heat, respectively; T_n' is temperature of condensed water; V is secondary steam flow rate for the evaporator; F_{01} and F_{02} are feed flow rate of the 5th and the 6th evaporator; cp_w is specific heat of water; for liquid material of the flash evaporator, F^s, ρ^s, T^s and cp^s are flow rate, density, temperature and specific heat, respectively; Q is the heat loss.

The evaporation process is based on heat transfer, so the optimization model needs to satisfy the mechanism balance relationships.

b: THE CONSTRAINT OF LIVE STEAM FLOW RATE

The live steam is the main source of heat for evaporation process. Under the condition of the actual live steam flow rate exceeding the acceptable value, it may condense the excess steam into water, resulting in a waste of steam. Nevertheless, insufficient concentration of sodium aluminate solution affects the product quality if live steam flow rate is low. So, the constraint of live steam flow rate can be expressed as:

$$V_{0,\min} \le V_0 \le V_{0,\max} \tag{30}$$

c: THE CONSTRAINT OF LIVE STEAM TEMPERATURE

The heat transfer in the evaporator is influenced by the live steam with high pressure and high temperature used directly for heating without condensation. Therefore, the steam pressure cannot be too large, and the live steam temperature constraint condition is:

$$T_{V0,\min} \le T_{V0} \le T_{V0,\max} \tag{31}$$

d: THE CONSTRAINT OF FEED FLOW RATE

The product concentration is affected by the fluctuation of feed flow rate. The heat of liquid material decreases with the increase of feed flow rate, which leads to the decrease of the product concentration. Moreover, to make sure the production efficiency and quality, the feed flow rate for the 6th and the 5th evaporator should be controlled within:

$$F_{01,\min} \le F_{01} \le F_{01,\max} \tag{32}$$

$$F_{02,\min} \le F_{02} \le F_{02,\max} \tag{33}$$

e: THE CONSTRAINT OF FEED TEMPERATURE

Under the condition of the constant negative pressure, the higher the feed temperature, the less heat is needed to evaporate the water in feed. Meanwhile, the change of the feed temperature affects the distribution of the effective temperature difference and product concentration and steam consumption. Thus, the feed temperature should be constrained within a certain range:

$$T_{0,\min} \le T_0 \le T_{0,\max} \tag{34}$$

Thus, the energy efficiency optimization based on the multi-objective is expressed as,

$$\begin{cases} \min\ J_1 = \min\left(1 - \eta_{ex}\right) = \min\left(1 - \dfrac{F_4^s \rho_4^s e_{m_4^s}}{V_0 e_{V0} + F_0 \rho_0 e_{m0}}\right) \\ \min\ J_2 = \min\left(\dfrac{V_0}{W_z}\right) = \min\left(\dfrac{V_0}{F_0 \rho_0 \left(1 - C_0 \rho_4^s / C_4^s \rho_0\right)}\right) \\ s.t.\ \ G\left(V_0, T_{V0}, F_{01}, F_{02}, T_0\right) = 0 \\ \quad F_{01,\min} \le F_{01} \le F_{01,\max} \\ \quad F_{02,\min} \le F_{02} \le F_{02,\max} \\ \quad V_{0,\min} \le V_0 \le V_{0,\max} \\ \quad T_{V0,\min} \le T_{V0} \le T_{V0,\max} \\ \quad T_{0,\min} \le T_0 \le T_{0,\max} \end{cases} \tag{35}$$

where $G(\cdot)$ is mechanism model; $V_{0,\min}$, $T_{V0,\min}$, $T_{0,\min}$, $F_{01,\min}$, $F_{02,\min}$ are the allowed minimum live steam flow rate and temperature, feed temperature and flow rate, respectively; $V_{0,\max}$, $T_{V0,\max}$, $T_{0,\max}$, $F_{01,\max}$, $F_{02,\max}$ are the allowed maximum live steam flow rate and temperature, feed temperature and flow rate, respectively.

The energy efficiency optimization for the evaporation process is a multi-objective complex optimization problem with inequality constraints and equality constraints. Hence, the multi-objective state transition algorithm (MOSTA) [55], [56] with its fast convergence and proper solution strategy is utilized to find the true Pareto solutions in this paper.

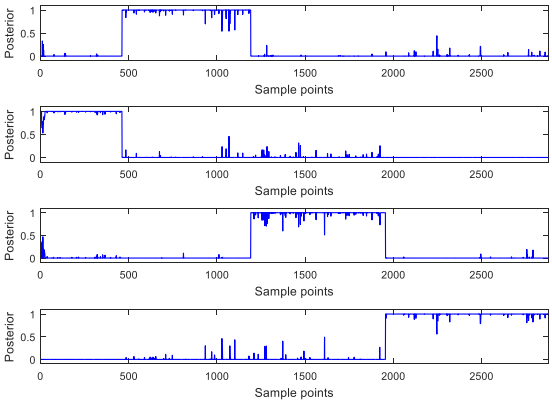

FIGURE 3. Probabilities of each sample for modes.

IV. RESULTS AND DISCUSSION

To demonstrate the availability and practicality of the proposed energy efficiency optimization method based on the novel data reconciliation, the simulation case and industrial application case are used to analyze and discuss, respectively.

A. SIMULATIONS AND ANALYSIS

First of all, a total of 2880 samples were collected in an acid-cleaning cycle for the evaporation process from an aluminium production plant in Zhengzhou, China, to evaluate the proposed novel data reconciliation method. First, in accordance with expert experience and prior knowledge, the experiment data is divided into four Gaussian components, namely four production modes, and the Gaussian mixture model is further constructed. The probabilities of each sample for modes are provided in Fig. 3. Moreover, the data reconciliation model with the mutual information and time-scale redundancy for the four modes are established, respectively. Then, 100 sets of process data are used to realize the online data reconciliation and improve the data quality.

In this case, the standard deviation from the measurements and the reconciliation results of measured variables are calculated and compared by means of multi-modes and different sub-mode data reconciliation results, as shown in Fig. 4. The Figs. 4(a)-4(i) mean the comparisons of the standard deviations for the feed temperature, the outlet liquid material flow rate and temperature of the 4th flash evaporator and the 6th evaporator, the live steam flow rate and temperature, the feed flow rate of the 6th and the 5th evaporator, the secondary steam temperature of the 4th flash evaporator, and the condensate water temperature, respectively. The y-axis is the calculated standard deviation, and the signs "M", "R", "R(1)", "R(2)", "R(3)", "R(4)" in x-axis represent the calculated standard deviation from measurements, reconciliations for multi-modes, reconciliations for the first mode, reconciliations for the second mode, reconciliations for the third mode, reconciliations for the fourth mode, respectively. Obviously,

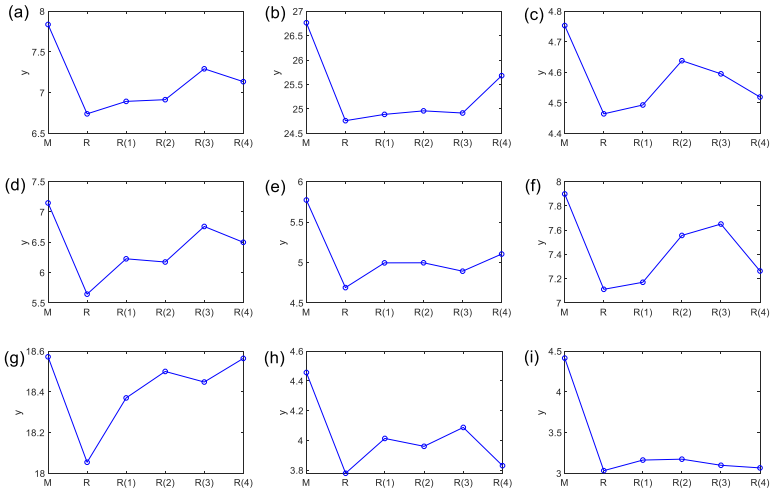

FIGURE 4. The comparisons of the standard deviation from measurements and reconciliations for the multimode and each sub-mode.

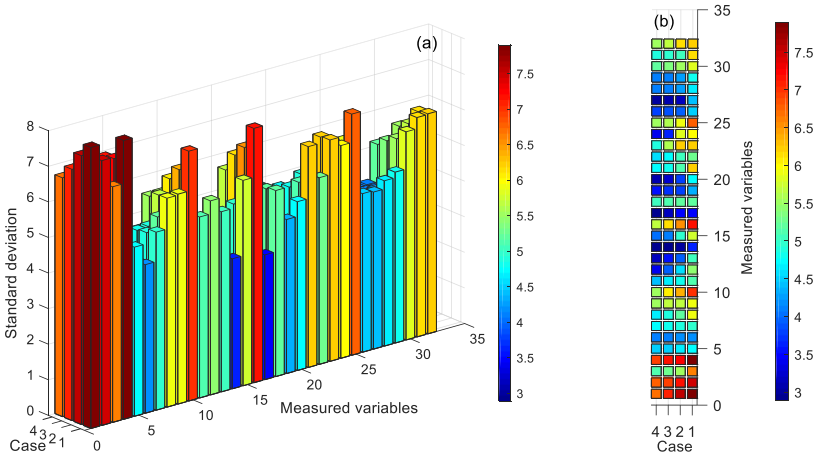

FIGURE 5. The standard deviation of different variables under different case.

the standard deviation calculated by the reconciliations is less than that calculated by the measurements, and the standard deviation from reconciliations in sub-mode is greater than that in multi-modes. Meanwhile, compared with the standard deviation from measurements, the standard deviation from reconciliations of condensate water temperature of the sixth evaporator, live steam flow rate and live steam temperature under multi-modes is decreased by 31.31%, 21.04%, 18.76%, respectively. The standard deviation of other six variables also decrease to varying degrees. It indicates that the proposed reconciliation method guarantees the measurements accuracy for the production process with the multi-modes characteristics.

Furthermore, to explain the superiority of the proposed data reconciliation method, the standard deviation obtained under the four cases are compared, including the measurements, the reconciliations from the reconciliation model without mode division, the reconciliations from the reconciliation model with diagonal matrix, and the reconciliations from the reconciliation model with mutual information matrix. For the different cases, the comparison results of the standard deviation for 34 measured variables are demonstrated in Fig. 5. Based on the comparative data, it should be noted that the standard deviations from reconciliations with multi-modes for different measured variables are obviously less than those of other cases, which is more conductive to reduce the measurement error.

In addition, the relative standard deviation (RSD) regarded as the evaluation indicator of reconciliation results is defined in Eq. (36). Fig. 6 shows the standard deviation and the corresponding relative standard deviation for multi-modes and different sub-mode. The reconciliation relative standard deviation of each variable is negative, which reflects that the standard deviation calculated from reconciliations is less than that from measurements, and the standard deviation calculated from reconciliations in multi-modes is less than that calculated under different sub-mode. In fact, the estimated interval for the reconciliations is narrower than the measurements. It follows that the proposed reconciliation method is

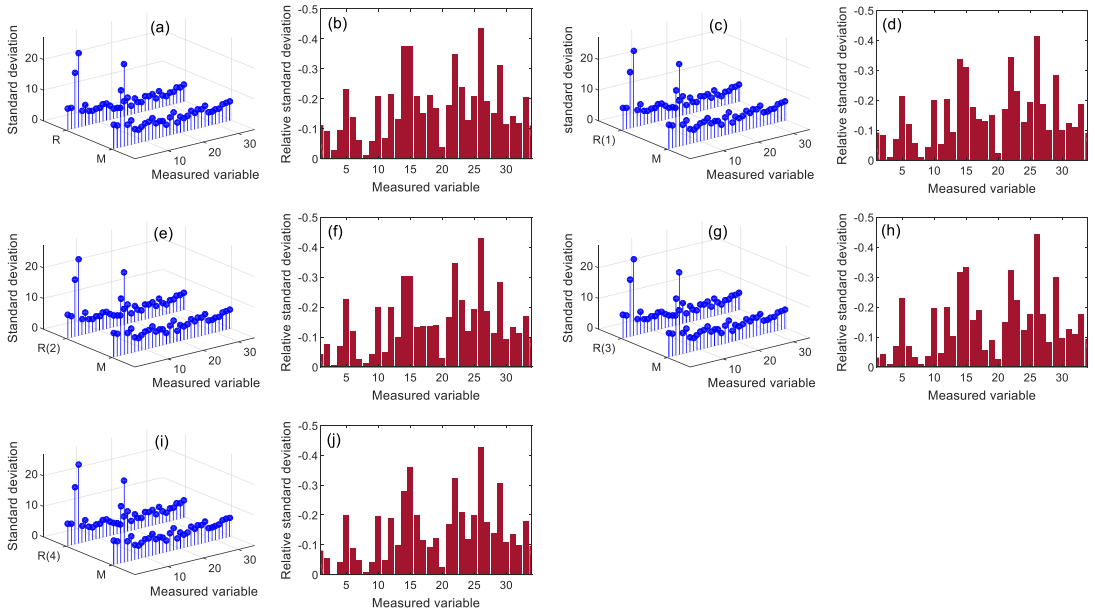

FIGURE 6. The standard deviation and the relative standard deviation for multi-modes and different sub-mode.

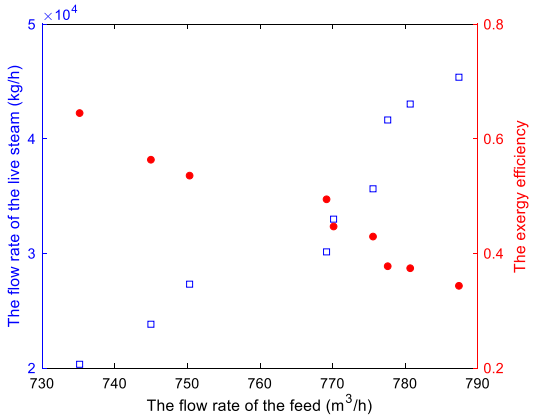

FIGURE 7. The effect of feed flow rate on live steam flow rate and exergy efficiency.

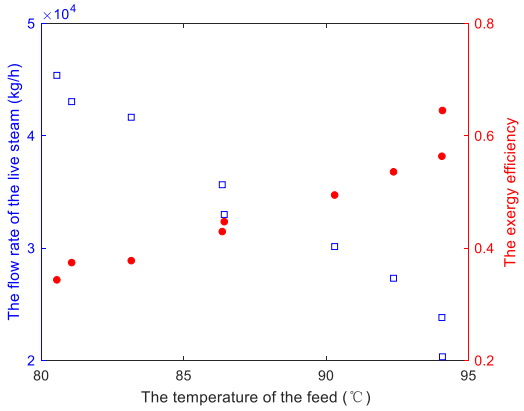

FIGURE 8. The effect of the feed temperature on live steam flow rate and exergy efficiency.

more remarkable and the obtained reconciliations are closer to the true value (36), as shown at the bottom of the next page.

Besides, to analyze the influence of operating parameters on steam consumption in an acid-cleaning cycle, the data of 9 days (from the 3rd to the 5th, from the 14th to the 16th, from the 26th to the 28th) were collected. The effect of feed flow rate on live steam flow rate and exergy efficiency is displayed in Fig. 7. Obviously, the increase in the feed flow rate results in the live steam flow rate increasing while the corresponding exergy efficiency decreasing. Moreover, the live steam flow rate is reduced and the exergy efficiency is increased by increasing the feed temperature, as shown in Fig. 8. Generally speaking, in the early stage of acid-cleaning cycle, there is no scaling with the highest operating efficiency, less steam consumption and smaller steam-water ratio. However, with the extension of acid-cleaning cycle, scaling in the evaporator occurs gradually, which directly affects the heat transfer of the evaporator. In the latter stage of acid-cleaning cycle, a lot of steam is consumed, resulting in larger steam-water ratio. The change of the steam-water ratio is shown in Fig. 9. From Fig. 9, in the early stage of acid-cleaning cycle, the steam-water ratio decreases first and then increases. When the evaporation system running after acid-cleaning, a large amount of steam is applied to ensure stable operation of production. This is lead to the fact that the steam-water ratio is high. After the system is stable, the steam-water ratio decreases and the required steam flow rate is reduced. In a word, it can be seen from these three figures that the changes of operating variables in the evaporation process have a comprehensive effect on exergy efficiency and steam-water ratio.

Subsequently, to assess the feasibility of the proposed energy efficiency optimization strategy, the comparison of MOSTA and nondominated sorting genetic algorithm II (NSGAII) [57] are carried out. Moreover, the parameters of the MOSTA are set as follows: α decreases periodi-

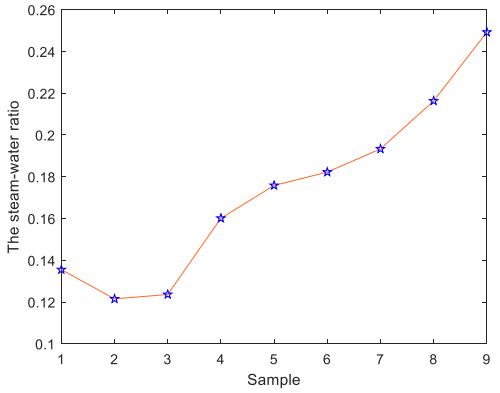

FIGURE 9. The change of the steam-water ratio.

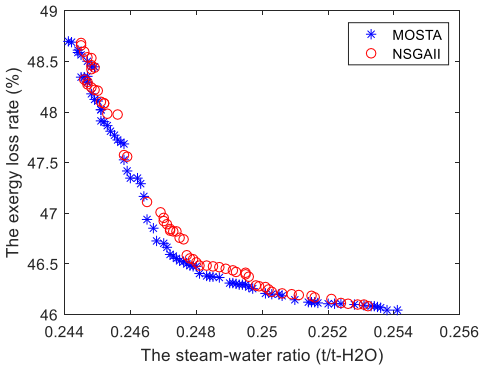

FIGURE 10. The Pareto profile for the steam-water ratio and the exergy loss rate.

cally in an exponential manner from 1 to 1e-4, β, γ and δ are set to 1. All parameters setting refer to the previous papers [58]. For the NSGAII, the crossover probability p_c is 0.9, the mutation probability p_m is $1/n$, where n is the number of the optimization variables. The Pareto profile for the steam-water ratio and the exergy loss rate obtained by the MOSTA and NSGAII is presented in Fig. 10. From Fig. 10, the length between the blue endpoints of the entire Pareto profile get by MOSTA is longer than that between the red endpoints, which means that the MOSTA has a better span metric. In addition, it is obvious that the blue marks are uniformly distributed on the entire Pareto profile, indicating that the MOSTA has better uniformity, namely, spacing metric. In contrast, the MOSTA can converge to the real Pareto profile with better distribution effectively and quickly.

Based on the above analysis, under the condition of stable operation of the system, the optimal results of the evaporation process are displayed with different methods in Table 2. From Table 2, the exergy efficiency and the steam-water ratio are contradictory, and the steam-water ratio reduces at the expense of the loss of the energy efficiency. It follows that

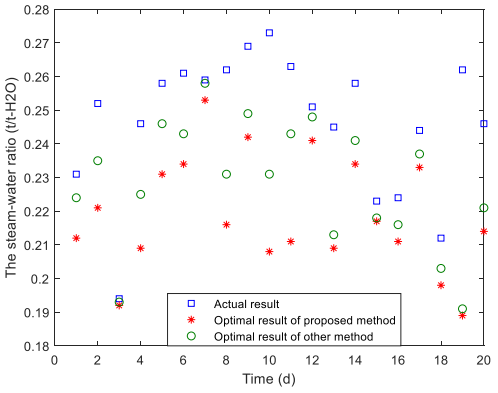

FIGURE 11. Comparisons of steam-water ratio for actual results, optimal results of proposed method and optimal results of other method.

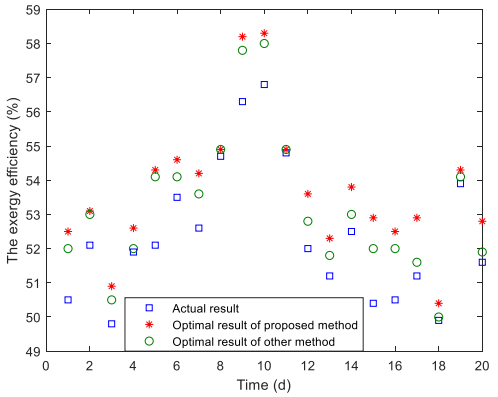

FIGURE 12. Comparisons of exergy efficiency for actual results, optimal results of proposed method and optimal results of other method.

FIGURE 13. The evaporation process of the alumina production in an aluminum metallurgical plant.

the optimized mass of live steam is lower than the actual production. In addition, the optimal exergy efficiency based on the proposed method and the optimal exergy efficiency of other method without data reconciliation are improved by 2.25% and 1.51%, respectively. In fact, Pareto solution set obtained by optimization provides a variety of options for different control objectives, which meets the operation

$$\text{RSD} = \frac{\text{reconciled standard deviation-measured standard deviation}}{\text{measured standard deviation}} \tag{36}$$

TABLE 2. The optimal parameters and performance indicators of energy efficiency optimization problem.

	Early stage of an acid-cleaning cycle			Middle stage of an acid-cleaning cycle			Later stage of an acid-cleaning cycle		
	Actual result	Optimal result of proposed method	Optimal results of other method	Actual result	Optimal result of proposed method	Optimal results of other method without DR	Actual result	Optimal result of proposed method	Optimal results of other method
The flow rate of the live steam	28.621	27.212	28.038	36.482	36.163	36.564	44.324	41.586	42.146
The temperature of the live steam	153.715	153.847	153.615	152.157	153.121	152.944	150.676	151.269	152.347
The temperature of the feed	84.975	84.837	84.154	84.211	84.572	83.656	83.946	82.651	83.684
The flow rate of the feed for the fifth evaporator	312.536	309.517	310.156	324.584	318.463	320.644	328.415	323.935	330.412
The flow rate of the feed for the sixth evaporator	455.672	450.156	451.254	449.154	446.088	446.135	461.255	440.841	448.548
The exergy efficiency	36.647	37.628	37.263	43.535	44.561	44.136	52.361	53.254	53.136
The steam-water ratio	0.152	0.146	0.148	0.203	0.196	0.199	0.251	0.247	0.248

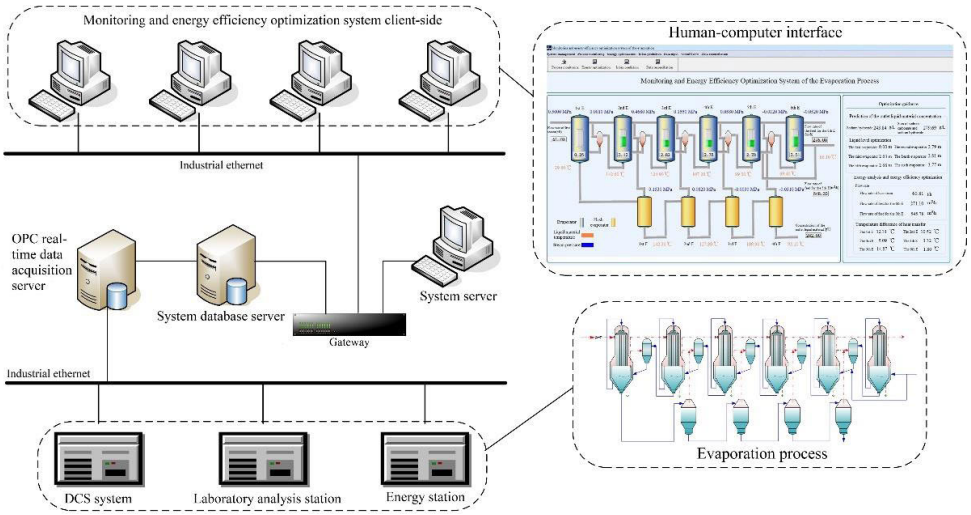

FIGURE 14. Structure of the monitoring and energy efficiency optimization system.

requirements under different working conditions. When the actual production process focuses on a certain index, Pareto optimal solution is selected from another scheme with a smaller index. If there is no special focus on the objective, a tradeoff between the exergy efficiency and the steam-water ratio is conducted. Obviously, the energy efficiency optimization approach put forward is more effective in ensuring low energy consumption and high exergy efficiency. Meanwhile, the process data of 20 days in an acid-cleaning cycle were obtained to optimize the steam-water ratio and the exergy efficiency meeting the actual working condition. Furthermore, the comparisons for optimal results of different methods are displayed in Fig. 11 and Fig. 12. It follows from the comparison results, the optimal results of the proposed method for the exergy efficiency compared with the actual results is improved by an average of about 2.45%, while the optimal results of other method for the exergy efficiency is improved by an average of about 1.52%, indicating that the proposed energy efficiency method has better performance on energy conservation and consumption reduction.

B. INDUSTRIAL APPLICATION

The monitoring and energy efficiency optimization system is performed and tested in the one of the aluminum metallurgical plant in China (Fig. 13). The proposed approach runs on an industrial computer with a 2.7GHz CPU and 4GB RAM in a Microsoft Windows 7 environment. A graphical human-computer monitoring interface software platform, including the functions of the important condition monitoring, data reconciliation, exergy analysis and optimization, etc., is developed for high-level optimization control, and the DCS system, laboratory analysis station and energy station are utilized for low-level data acquisition. The platform is implemented through using Microsoft Visual C++,

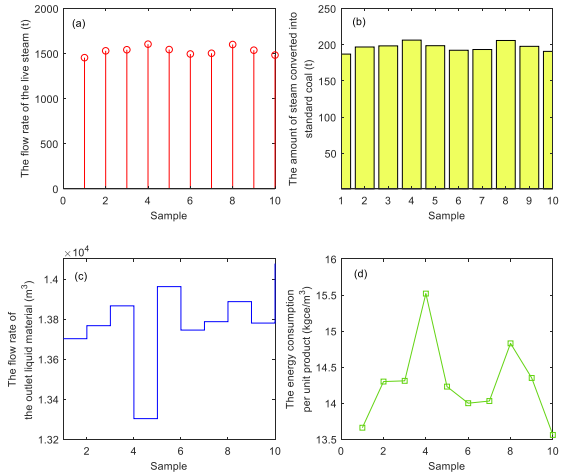

FIGURE 15. The energy consumption index of the 10 days before the system.

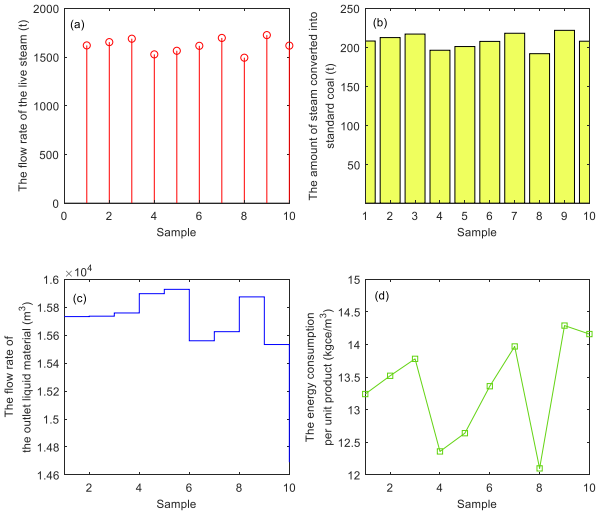

FIGURE 16. The energy consumption index of the 10 days after the system.

Microsoft SQL Server, and provided production guidance for the actual plant, presented as Fig. 14.

To exhibit the superiority of the proposed strategy and the benefit of the energy efficiency optimization system, the energy consumption per unit product as the main evaluation index is used for analysis of energy conservation. The data of the 10 days before the system and the data of the 10 days after the system are collected to compare the performance of the proposed strategy applied in industrial plant. According to the calculation general rule of the comprehensive energy consumption (GB/T 2589-2008), steam is converted into standard coal by the conversion coefficient of standard coal which is 0.1286. To compare the energy consumption of the 10 days before and after the energy efficiency system, the details for the live steam flow rate, an amount of steam converted into standard coal, the outlet liquid material flow rate, and the energy consumption per unit product are demonstrated in Fig. 15 and Fig. 16. It can be seen intuitively that the specific numerical changes of energy consumption indicators of the 10 days before and the 10 days after the system implementation.

It follows that the total amount of energy consumption converted into standard coal is 1967.84tce, the total outlet liquid material flow rate is 137876m^3, the comprehensive energy consumption per unit product is 14.27kgce/m^3 before the system. Nevertheless, after the system, the total amount of energy consumption converted into standard coal is 2084.22tce, the total outlet liquid material flow rate is 156336m^3, the comprehensive energy consumption per unit product is 13.33kgce/m^3. Hence, for the system, the energy consumption is reduced by 6.58% after the monitoring and energy efficiency optimization system of the evaporation process is applied for actual production. Clearly, the automation level of production technology is improved and the production process is optimized. In addition, it also achieves the purpose of energy conservation and consumption reduction.

V. CONCLUSION

This paper put forward an energy efficiency optimization strategy based on a novel data reconciliation for improving energy utilization and reducing energy consumption. The multi-features material flow information is divided into several sub-mode by the Gaussian mixture model. In addition, the critical variable introduced to improve the data redundancy is applied for the local data reconciliation modeling with the mutual information, and the hypothesis testing is used to evaluate the data reconciliation results. Moreover, exergy analysis is employed for energy utilization of production equipment according to a case study about evaporation process. Subsequently, an energy efficiency optimization model based on performance indicator is established and is solved by the MOSTA. Finally, the simulations and industrial application illustrate that the proposed energy efficiency optimization method has better effectiveness and superiority for energy-saving and cost-reducing in terms of the exergy efficiency and the steam-water ratio. Besides, the process measurements preprocessed by data reconciliation can better obtain effective production information, and further improve the accuracy of optimization and the production efficiency of alumina industry. Thus, the energy consumption of evaporation production can be reduced by more than 2%, which significantly improves the energy efficiency of the evaporation production.

Furthermore, in the production process of alumina, the concentration of the feed for the evaporation process is determined by the preceding decomposition process, and the live steam used for heating is provided by the thermal power plant. In addition, the product quality of the evaporation process is determined by the production requirements of the subsequent digestion process. Due to the limitation of detection conditions at present, it is difficult for the production operation of evaporation process to track the production changes of the preceding and the subsequent processes in time. When multiple production processes in series, it is of great significant

to how to improve energy efficiency of the whole alumina production process under the premise that multi-processes have the characteristics of multiple working conditions and nonlinearity.

REFERENCES

[1] Y. M. Han, C. Long, Z. Q. Geng, Q. X. Zhu, and Y. H. Zhong, "A novel DEACM integrating affinity propagation for performance evaluation and energy optimization modeling: Application to complex petrochemical industries," *Energy Convers. Manage.*, vol. 183, pp. 349–359, Mar. 2019.

[2] H. Z. Wang, Y. Y. Liu, B. Zhou, C. B. Li, G. Z. Cao, N. Voropai, and E. Barakhtenko, "Taxonomy research of artificial intelligence for deterministic solar power forecasting," *Energy Convers. Manage.*, vol. 214, Jun. 2020, Art. no. 112909.

[3] Z. Geng, R. Zeng, Y. Han, Y. Zhong, and H. Fu, "Energy efficiency evaluation and energy saving based on DEA integrated affinity propagation clustering: Case study of complex petrochemical industries," *Energy*, vol. 179, pp. 863–875, Jul. 2019.

[4] D. Fernández, C. Pozo, R. Folgado, L. Jiménez, and G. Guillén-Gosálbez, "Productivity and energy efficiency assessment of existing industrial gases facilities via data envelopment analysis and the malmquist index," *Appl. Energy*, vol. 212, pp. 1563–1577, Feb. 2018.

[5] L. Zhu and J. Chen, "Energy efficiency evaluation and prediction of large-scale chemical plants using partial least squares analysis integrated with Gaussian process models," *Energy Convers. Manage.*, vol. 195, pp. 690–700, Sep. 2019.

[6] Y. Liu, Q. Cheng, Y. Gan, Y. Wang, Z. Li, and J. Zhao, "Multi-objective optimization of energy consumption in crude oil pipeline transportation system operation based on exergy loss analysis," *Neurocomputing*, vol. 332, pp. 100–110, Mar. 2019.

[7] Y. Han, R. Zhou, Z. Geng, J. Bai, B. Ma, and J. Fan, "A novel data envelopment analysis cross-model integrating interpretative structural model and analytic hierarchy process for energy efficiency evaluation and optimization modeling: Application to ethylene industries," *J. Cleaner Prod.*, vol. 246, Feb. 2020, Art. no. 118965.

[8] N. Ha Hoang, D. Rodrigues, and D. Bonvin, "Revisiting the concept of extents for chemical reaction systems using an enthalpy balance," *Comput. Chem. Eng.*, vol. 136, May 2020, Art. no. 106652.

[9] A. Sakly and F. Ben Nejma, "Heat and mass transfer of combined forced convection and thermal radiation within a channel: Entropy generation analysis," *Appl. Thermal Eng.*, vol. 171, May 2020, Art. no. 114903.

[10] M. I. Afridi, M. Qasim, and O. D. Makinde, "Entropy generation due to heat and mass transfer in a flow of dissipative elastic fluid through a porous medium," *J. Heat Transf.*, vol. 141, no. 2, Feb. 2019, Art. no. 022002.

[11] S. Zhou, X. Liu, Y. Bian, and S. Shen, "Energy, exergy and exergoeconomic analysis of a combined cooling, desalination and power system," *Energy Convers. Manage.*, vol. 218, Aug. 2020, Art. no. 113006.

[12] M. Rangasamy, G. Duraisamy, and N. Govindan, "A comprehensive parametric, energy and exergy analysis for oxygenated biofuels based dual-fuel combustion in an automotive light duty diesel engine," *Fuel*, vol. 277, Oct. 2020, Art. no. 118167.

[13] A. Ebrahimi and M. Ziabasharhagh, "Energy and exergy analyses of a novel integrated process configuration for tri-generation heat, power and liquefied natural gas based on biomass gasification," *Energy Convers. Manage.*, vol. 209, Apr. 2020, Art. no. 112624.

[14] Y. Liu, X. Y. Xiang, Q. L. Cheng, X. X. Wang, and T. Yu, "Optimised operation of multi–level exergy analysis for complicated production systems," *Int. J. Exergy*, vol. 13, no. 2, pp. 201–219, 2013.

[15] Z. H. Li and B. Hua, "Modeling and optimizing for heat exchanger networks synthesis based on expert system and exergo—Economic objective function," *Comput. Chem. Eng.*, vol. 24, nos. 2–7, pp. 1223–1228, Jul. 2000.

[16] J. U. Ahamed, R. Saidur, and H. H. Masjuki, "A review on exergy analysis of vapor compression refrigeration system," *Renew. Sustain. Energy Rev.*, vol. 15, no. 3, pp. 1593–1600, Apr. 2011.

[17] U. Safder, P. Ifaei, and C. Yoo, "A novel approach for optimal energy recovery using pressure retarded osmosis technology: Chemical exergy pinch analysis–case study in a sugar mill plant," *Energy Convers. Manage.*, vol. 213, Jun. 2020, Art. no. 112810.

[18] O. Arslan, "Performance analysis of a novel heat recovery system with hydrogen production designed for the improvement of boiler effectiveness," *Int. J. Hydrogen Energy*, vol. 46, no. 10, pp. 7558–7572, Feb. 2021.

[19] J. Sun, F. Wang, T. Ma, H. Gao, P. Wu, and L. Liu, "Energy and exergy analysis of a five-column methanol distillation scheme," *Energy*, vol. 45, no. 1, pp. 696–703, Sep. 2012.

[20] R. Fang, J. Li, and T. T. Wu, "Energy saving and high production efficiency of cold rolled hot-dip galvanizing annealing furnace," *Surf. Tech.*, vol. 45, pp. 42–48, 2016.

[21] D. Peinado, M. de Vega, N. García-Hernando, and C. Marugán-Cruz, "Energy and exergy analysis in an asphalt plant's rotary dryer," *Appl. Thermal Eng.*, vol. 31, nos. 6–7, pp. 1039–1049, May 2011.

[22] P. Ahmadi, M. A. Rosen, and I. Dincer, "Multi-objective exergy-based optimization of a polygeneration energy system using an evolutionary algorithm," *Energy*, vol. 46, no. 1, pp. 21–31, Oct. 2012.

[23] F. Suleman, I. Dincer, and M. Agelin-Chaab, "Energy and exergy analyses of an integrated solar heat pump system," *Appl. Thermal Eng.*, vol. 73, no. 1, pp. 559–566, Dec. 2014.

[24] H. S. Hamut, I. Dincer, and G. F. Naterer, "An exergoeconomic analysis of hybrid electric vehicle thermal management systems," *J. Thermal Sci. Eng. Appl.*, vol. 6, no. 2, pp. 187–196, Jun. 2014.

[25] N. Javani, I. Dincer, G. F. Naterer, and B. S. Yilbas, "Exergy analysis and optimization of a thermal management system with phase change material for hybrid electric vehicles," *Appl. Thermal Eng.*, vol. 64, nos. 1–2, pp. 471–482, Mar. 2014.

[26] J. Jannatkhah, B. Najafi, and H. Ghaebi, "Energy and exergy analysis of combined ORC–ERC system for biodiesel-fed diesel engine waste heat recovery," *Energy Convers. Manage.*, vol. 209, Apr. 2020, Art. no. 112658.

[27] F. C. N. Silva, D. Flórez-Orrego, and S. de Oliveira Junior, "Exergy assessment and energy integration of advanced gas turbine cycles on an offshore petroleum production platform," *Energy Convers. Manage.*, vol. 197, Oct. 2019, Art. no. 111846.

[28] T. Kowalczyk, J. Badur, and M. Bryk, "Energy and exergy analysis of hydrogen production combined with electric energy generation in a nuclear cogeneration cycle," *Energy Convers. Manage.*, vol. 198, Oct. 2019, Art. no. 111805.

[29] A. S. Gutiérrez, J. B. C. Martínez, and C. Vandecasteele, "Energy and exergy assessments of a lime shaft kiln," *Appl. Thermal Eng.*, vol. 51, nos. 1–2, pp. 273–280, Mar. 2013.

[30] Y. Han, Q. Zeng, Z. Geng, and Q. Zhu, "Energy management and optimization modeling based on a novel fuzzy extreme learning machine: Case study of complex petrochemical industries," *Energy Convers. Manage.*, vol. 165, pp. 163–171, Jun. 2018.

[31] Z. Zeng, M. Hong, J. Li, Y. Man, H. Liu, Z. Li, and H. Zhang, "Integrating process optimization with energy-efficiency scheduling to save energy for paper mills," *Appl. Energy*, vol. 225, pp. 542–558, Sep. 2018.

[32] G. Thiele, O. Heimann, K. Grabowski, and J. Krüger, "Framework for energy efficiency optimization of industrial systems based on the control layer model," *Procedia Manuf.*, vol. 33, pp. 414–421, Jan. 2019.

[33] S. X. Gong, C. Shao, and L. Zhu, "An energy efficiency integration optimization scheme for ethylene production with respect to multiple working conditions," *Energy*, vol. 182, pp. 280–295, Sep. 2019.

[34] T. Luna, J. Ribau, D. Figueiredo, and R. Alves, "Improving energy efficiency in water supply systems with pump scheduling optimization," *J. Cleaner Prod.*, vol. 213, pp. 342–356, Mar. 2019.

[35] A. Kaab, M. Sharifi, H. Mobli, A. Nabavi-Pelesaraei, and K.-W. Chau, "Use of optimization techniques for energy use efficiency and environmental life cycle assessment modification in sugarcane production," *Energy*, vol. 181, pp. 1298–1320, Aug. 2019.

[36] B. Zhao, Y. Ren, D. Gao, L. Xu, and Y. Zhang, "Energy utilization efficiency evaluation model of refining unit based on contourlet neural network optimized by improved grey optimization algorithm," *Energy*, vol. 185, pp. 1032–1044, Oct. 2019.

[37] D. R. Kuehn and H. Davidson, "Computer control II. Mathematics of control," *Chem. Eng. Prog.*, vol. 57, no. 6, pp. 44–47, 1961.

[38] J. Chebeir, Z. T. Webb, and J. A. Romagnoli, "An environment for topology analysis and data reconciliation of the pre-heat train in an industrial refinery," *Appl. Thermal Eng.*, vol. 147, pp. 623–635, Jan. 2019.

[39] X. Yang, Q. Yang, and W. Dong, "Aeroengine data reconciliation model based on cooperative working equations," *Energy*, vol. 186, Nov. 2019, Art. no. 115914.

[40] S. Guo, P. Liu, and Z. Li, "Estimation of exhaust steam enthalpy and steam wetness fraction for steam turbines based on data reconciliation with characteristic constraints," *Comput. Chem. Eng.*, vol. 93, pp. 25–35, Oct. 2016.

[41] S. Guo, P. Liu, and Z. Li, "Data reconciliation for the overall thermal system of a steam turbine power plant," *Appl. Energy*, vol. 165, pp. 1037–1051, Mar. 2016.
[42] X. Jiang, P. Liu, and Z. Li, "A data reconciliation based framework for integrated sensor and equipment performance monitoring in power plants," *Appl. Energy*, vol. 134, pp. 270–282, Dec. 2014.
[43] S. Xie, C. Yang, X. Yuan, X. Wang, and Y. Xie, "A novel robust data reconciliation method for industrial processes," *Control Eng. Pract.*, vol. 83, pp. 203–212, Feb. 2019.
[44] Z. Zhang, Z. Shao, and J. Chen, "Programming strategies of sequential incremental-scale subproblems for large scale data reconciliation and parameter estimation with multi-operational conditions," *Ind. Eng. Chem. Res.*, vol. 54, no. 21, pp. 5697–5709, Jun. 2015.
[45] Z. Zhang, Y.-Y. Chuang, and J. Chen, "Using clustering based logical equation set to decompose large scale chemical processes for parallel solving data reconciliation and parameter estimation problem," *Chem. Eng. Res. Design*, vol. 120, pp. 396–409, Apr. 2017.
[46] S. Xie, C. Yang, X. Yuan, X. Wang, and Y. Xie, "Layered online data reconciliation strategy with multiple modes for industrial processes," *Control Eng. Pract.*, vol. 77, pp. 63–72, Aug. 2018.
[47] X. F. Yuan, Z. Q. Ge, and Z. H. Song, "Soft sensor model development in multiphase/multimode processes based on Gaussian mixture regression," *Chemometrics Intell. Lab.*, vol. 138, pp. 109–197, Nov. 2014.
[48] J. Yu, "Online quality prediction of nonlinear and non-Gaussian chemical processes with shifting dynamics using finite mixture model based Gaussian process regression approach," *Chem. Eng. Sci.*, vol. 82, pp. 22–30, Sep. 2012.
[49] J. Yu, "Multiway Gaussian mixture model based adaptive kernel partial least squares regression method for soft sensor estimation and reliable quality prediction of nonlinear multiphase batch processes," *Ind. Eng. Chem. Res.*, vol. 51, no. 40, pp. 13227–13237, Oct. 2012.
[50] S. W. Choi, J. H. Park, and I.-B. Lee, "Process monitoring using a Gaussian mixture model via principal component analysis and discriminant analysis," *Comput. Chem. Eng.*, vol. 28, no. 8, pp. 1377–1387, Jul. 2004.
[51] J. Yu and S. J. Qin, "Multimode process monitoring with Bayesian inference-based finite Gaussian mixture models," *AIChE J.*, vol. 54, no. 7, pp. 1811–1829, Jul. 2008.
[52] S. Verron, T. Tiplica, and A. Kobi, "Fault detection and identification with a new feature selection based on mutual information," *J. Process Control*, vol. 18, no. 5, pp. 479–490, Jun. 2008.
[53] Y. Zhang, M. Sun, J. Hong, X. Han, J. He, W. Shi, and X. Li, "Environmental footprint of aluminum production in China," *J. Cleaner Prod.*, vol. 133, pp. 1242–1251, Oct. 2016.
[54] H. Kretzschmar, U. Overhoff, and W. Wagner, *Extended IAPWS-IF97 Steam Tables*. Berlin, Germany: Springer, 2007.
[55] J. Han, C. Yang, X. Zhou, and W. Gui, "Dynamic multi-objective optimization arising in iron precipitation of zinc hydrometallurgy," *Hydrometallurgy*, vol. 173, pp. 134–148, Nov. 2017.
[56] X. Zhou, J. Zhou, C. Yang, and W. Gui, "Set-point tracking and multi-objective optimization-based PID control for the goethite process," *IEEE Access*, vol. 6, pp. 36683–36698, 2018.
[57] K. Deb, A. Pratap, S. Agarwal, and T. Meyarivan, "A fast and elitist multiobjective genetic algorithm: NSGA-II," *IEEE Trans. Evol. Comput.*, vol. 6, no. 2, pp. 182–197, Apr. 2002.
[58] X. Zhou, C. Yang, and W. Gui, "A statistical study on parameter selection of operators in continuous state transition algorithm," *IEEE Trans. Cybern.*, vol. 49, no. 10, pp. 3722–3730, Oct. 2019.

SEN XIE received the B.Eng. degree in electrical engineering and automation from the Hunan University of Technology, China, in 2011, the M.Eng. degree in control theory and control engineering from Liaoning Technical University, China, in 2014, and the Ph.D. degree in control science and engineering from Central South University, China, in 2018. She is currently a Postdoctoral Researcher with Shenzhen University, China. Her research interests include modeling and optimal control of complex industrial process, data processing, and intelligent analysis.

HUAIZHI WANG (Member, IEEE) received the B.Eng. and M.Eng. degrees in control science and engineering from Shenzhen University, Shenzhen, China, in 2009 and 2012, respectively, and the Ph.D. degree in electrical engineering from the South China University of Technology, Guangzhou, China, in 2015. From 2014 to 2015, he was a Research Assistant with the Department of Electrical Engineering, The Hong Kong Polytechnic University, Hong Kong. He is currently an Assistant Professor with Shenzhen University. His research interest includes automatic generation control in cyber physical power systems.

JIANCHUN PENG received the B.S. and M.S. degrees in electrical engineering from Chongqing University, Chongqing, China, in 1986 and 1989, respectively, and the Ph.D. degree in electrical engineering from Hunan University, Hunan, China, in 1998. He was a Visiting Professor with Arizona State University, Tempe, AZ, USA, from 2002 to 2003, and with Brunel University, London, U.K., in 2006. He is currently a Professor with Shenzhen University and the Director of the Department of Control Science and Engineering. His research interests include electricity markets and power system optimal operation and control.